



Statens vegvesen

Ferry free E39 –Fjord crossings Bjørnafjorden

304624

Rev.	Publish date	Description	Made by	Checked by	Project appro.	Client appro.
0	18.09.2019	Final issue	PGS	MAS	SEJ	
Client	 Statens vegvesen					
Contractor	Contract no.: 18/91094					
AAS-JAKOBSEN COWI Multiconsult <small>JOHS HOLT AkerSolutions entail NGI DISSING+WITLING architecture als mossmaritime</small>						

Document name:

Skew wind sensitivity study

Document no.:

SBJ-32-C5-AMC-20-TN-001

Rev.:

0

Pages:

20

MEMO

PROJECT	Concept development, floating bridge E39 Bjørnafjorden	DOCUMENT CODE	SBJ-32-C5-AMC-20-TN-001
CLIENT	Statens vegvesen	ACCESSIBILITY	Restricted
SUBJECT	Skew wind sensitivity study	PROJECT MANAGER	Svein Erik Jakobsen
TO	Statens vegvesen	PREPARED BY	Pål Grøthe Sandnes, Mitja Papinutti
COPY TO		RESPONSIBLE UNIT	AMC

SUMMARY

In order to consider the skew wind effects on a slender structure, the *Entail* in-house wind code has been modified to accept 2D aerodynamic coefficients dependant on skew angle and angle of attack. Based on the modified wind code, a benchmarking on Bjørnafjorden K12 concept has been performed. A preliminary study of the benchmark results show that the skew wind effects may be important for some responses, depending on the excited modes. Further investigations are needed in order to fully understand the effect and importance on a general basis, both in terms of the input (aerodynamic coefficients) and the bridge response.

0	18.09.2019	Final issue	P. G. Sandnes	M. Storheim	S. E. Jakobsen
REV.	DATE	DESCRIPTION	PREPARED BY	CHECKED BY	APPROVED BY

1 Background

During the project the Client raised some concern regard the effect of skew wind coefficients on the bridge response based on an article¹. To investigate the subject further, a small modification to the *Entail* in-house wind code was implemented in order to consider the skew wind effects in the buffeting wind load calculation.

¹ Buffeting response of long-span cable-supported bridge under skew winds, L.D. Zhu & Y.L. Xu, 2004

2 Theory

2.1 Notations

α	Angle of attack
β	Skew angle
\vec{F}_W	Aerodynamic force vector in the wind aligned coordinate system
\vec{F}_N	Aerodynamic force vector in the node orientation coordinate system
\vec{M}_W	Aerodynamic moment vector in the wind aligned coordinate system
\vec{M}_N	Aerodynamic moment vector in the node orientation coordinate system
\vec{U}_G	Wind speed vector in the global coordinate system
\vec{U}_W	Wind speed vector in the wind aligned coordinate system
\vec{C}_F	Aerodynamic force coefficient vector in the wind aligned coordinate system
\vec{C}_M	Aerodynamic moment coefficient vector in the wind aligned coordinate system
$T_{G \rightarrow W}$	Transformation matrix from global to wind aligned coordinate system
$T_{G \rightarrow N}$	Transformation matrix from global to node orientation coordinate system
$T_{W \rightarrow N}$	Transformation matrix from wind aligned to node orientation coordinate system

2.2 Coordinate systems

Three coordinate systems are used in the aerodynamic skew wind model (as shown in Figure 2-1).

1. (G) Global coordinate system (fixed in space)
2. (W) Wind aligned coordinate system
3. (N) Node oriented coordinate system

The wind speed vectors are provided in the global coordinate system. The transformation matrices are defined such that vectors can be transformed between the 3 coordinate systems. The transformation matrices are orthogonal. The inverse of the transformation matrices is therefore identical to its transpose ($T_{2 \rightarrow 1} = T_{1 \rightarrow 2}^T$).

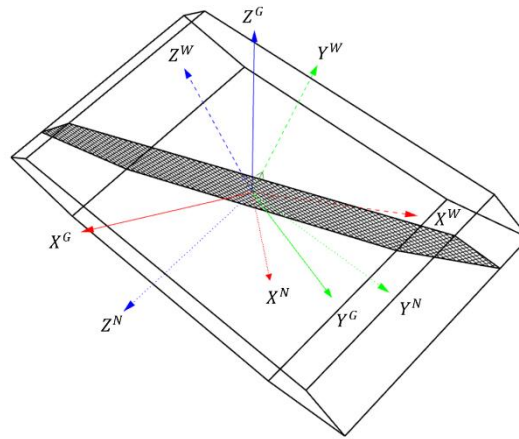


Figure 2-1 Illustration of the various coordinate systems.

2.2.1 Node orientation coordinate system (N)

The node orientation coordinate system (N), illustrated in Figure 2-1 with dotted lines, is defined from 3 intrinsic (Z-Y-Z) rotations. The transformation matrix $\mathbf{T}_{G \rightarrow N}$ represents the transformation from the global coordinate system G to N. The sine and cosine of the rotation angles are denoted S and C.

$$\vec{X}_N = \mathbf{T}_{G \rightarrow N} \cdot \vec{X}_G = \mathbf{T}_{2 \rightarrow N} \cdot \mathbf{T}_{1 \rightarrow 2} \cdot \mathbf{T}_{G \rightarrow 1} \cdot \vec{X}_G$$

$$\mathbf{T}_{G \rightarrow 1} = \begin{bmatrix} C1 & S1 & 0 \\ -S1 & C1 & 0 \\ 0 & 0 & 1 \end{bmatrix} \quad \text{Rotation about } Z_G$$

$$\mathbf{T}_{1 \rightarrow 2} = \begin{bmatrix} C2 & 0 & -S2 \\ 0 & 1 & 0 \\ S2 & 0 & C2 \end{bmatrix} \quad \text{Rotation about } Y_1$$

$$\mathbf{T}_{2 \rightarrow N} = \begin{bmatrix} C3 & S3 & 0 \\ -S3 & C3 & 0 \\ 0 & 0 & 1 \end{bmatrix} \quad \text{Rotation about } Z_2$$

2.2.2 Wind aligned coordinate system (W)

The wind aligned coordinate system W, illustrated in Figure 2-1 with dashed lines, is defined from 3 intrinsic (Z-Y-X) rotations. The transformation matrix $\mathbf{T}_{G \rightarrow W}$ represents the transformation from the global coordinate system G to W. The sine and cosine of the rotation angles are denoted S and C.

$$\vec{X}_W = \mathbf{T}_{G \rightarrow W} \cdot \vec{X}_G = \mathbf{T}_{2 \rightarrow W} \cdot \mathbf{T}_{1 \rightarrow 2} \cdot \mathbf{T}_{G \rightarrow 1} \cdot \vec{X}_G$$

$$\mathbf{T}_{G \rightarrow 1} = \begin{bmatrix} C1 & S1 & 0 \\ -S1 & C1 & 0 \\ 0 & 0 & 1 \end{bmatrix} \quad \text{Rotation about } Z_G$$

$$\mathbf{T}_{1 \rightarrow 2} = \begin{bmatrix} C2 & 0 & S2 \\ 0 & 1 & 0 \\ -S2 & 0 & C2 \end{bmatrix} \quad \text{Rotation about } Y_1$$

$$\mathbf{T}_{2 \rightarrow W} = \begin{bmatrix} 1 & 0 & 0 \\ 0 & C3 & S3 \\ 0 & -S3 & C3 \end{bmatrix} \quad \text{Rotation about } X_2$$

The first rotation angle is defined as $\arctan2(V, U)$ and the second rotation angle is defined as $\arctan2(W, \sqrt{U^2 + V^2})$ where U , V and W are the *relative* wind speed vector components in the global coordinate system. The third rotation depends on the node orientation and is performed to ensure that the X-axis of the node coordinate system is co-planar with the XZ-plane of the wind aligned coordinate system.

Forces and moments calculated in the wind aligned coordinate system is thus transformed to the node orientation coordinate system as following

$$\begin{aligned} \vec{F}_N &= \mathbf{T}_{W \rightarrow N} \cdot \vec{F}_W = \mathbf{T}_{G \rightarrow N} \cdot \mathbf{T}_{W \rightarrow G} \cdot \vec{F}_W \\ \vec{M}_N &= \mathbf{T}_{W \rightarrow N} \cdot \vec{M}_W = \mathbf{T}_{G \rightarrow N} \cdot \mathbf{T}_{W \rightarrow G} \cdot \vec{M}_W \end{aligned}$$

2.3 Aerodynamic buffeting theory

The skew wind was implemented both with nonlinear and linear buffeting theory.

2.3.1 Non-linear model

The instantaneous aerodynamic force and moment vectors are calculated at each time step in the dynamic wind aligned coordinate system.

$$\begin{aligned} \vec{F}_W &= 1/2 \rho |\vec{U}|^2 \cdot \vec{C}_F(\alpha, \beta) \\ \vec{M}_W &= 1/2 \rho |\vec{U}|^2 \cdot \vec{C}_M(\alpha, \beta) \\ \vec{C}_F(\alpha, \beta) &= \begin{bmatrix} C_{FX}(\alpha, \beta) \\ C_{FY}(\alpha, \beta) \\ C_{FZ}(\alpha, \beta) \end{bmatrix}, \vec{C}_M(\alpha, \beta) = \begin{bmatrix} C_{MX}(\alpha, \beta) \\ C_{MY}(\alpha, \beta) \\ C_{MZ}(\alpha, \beta) \end{bmatrix} \end{aligned}$$

Angle of attack α and skew angle β are functions of the wind and node orientation as shown in the illustration below. $|\vec{U}|$ is the magnitude of the instantaneous relative wind speed vector, invariant of the coordinate system.

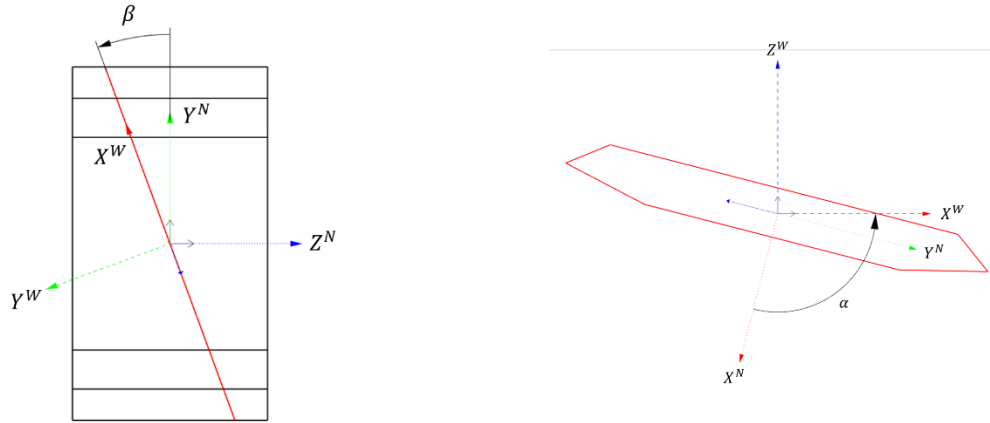


Figure 2-2 2D view of bridge, top view (left) with bridge axis in the horizontal direction and side view (right) with bridge axis normal to the figure.

2.3.2 Linear model

The instantaneous linearized aerodynamic forces and moments are calculated at each time step in the static wind aligned coordinate system (W).

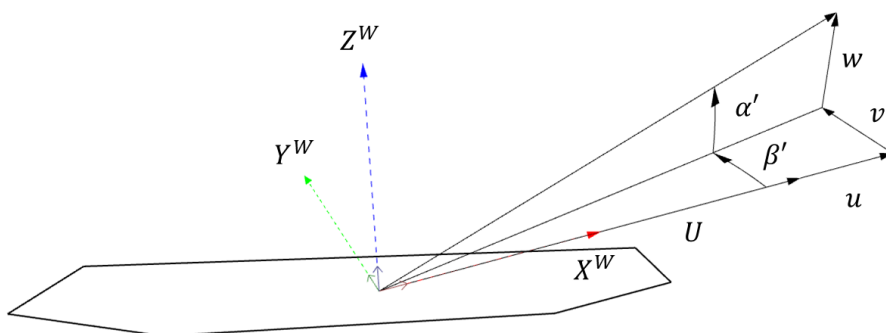
First the instantaneous *relative* wind speed vector is transformed from the global coordinate system (G) to the static wind aligned coordinate system (W), i.e. the wind coordinate system from the static simulation step.

$$\vec{U}_W = \begin{bmatrix} U + u \\ v \\ w \end{bmatrix} = \mathbf{T}_{G \rightarrow W} \cdot \vec{U}_G$$

Then the magnitude of the instantaneous *relative* wind speed vector is linearized in the static wind aligned coordinate system:

$$|\vec{U}|^2 = |\vec{U}_W|^2 = (U + u)^2 + v^2 + w^2 \approx U^2 \left(1 + 2 \frac{u}{U} \right)$$

The aerodynamic coefficients are linearized as in the below figure.



A linear approximation of the aerodynamic coefficients was defined within the fluctuating range. The instantaneous angle of attack and skew angle was split into a mean and fluctuating part.

$$\alpha = \bar{\alpha} + \alpha', \beta = \bar{\beta} + \beta'$$

$$\vec{C}_F(\alpha, \beta) \approx \vec{C}_F(\bar{\alpha}, \bar{\beta}) + \alpha' \partial_{\alpha} \vec{C}_F(\bar{\alpha}, \bar{\beta}) + \beta' \partial_{\beta} \vec{C}_F(\bar{\alpha}, \bar{\beta})$$

$$\vec{C}_M(\alpha, \beta) \approx \vec{C}_M(\bar{\alpha}, \bar{\beta}) + \alpha' \partial_{\alpha} \vec{C}_M(\bar{\alpha}, \bar{\beta}) + \beta' \partial_{\beta} \vec{C}_M(\bar{\alpha}, \bar{\beta})$$

If the fluctuating wind components u, v and w are much smaller than the mean wind component U , the following assumptions holds

$$\alpha' = \text{atan} \frac{w}{U+u} \approx \frac{w}{U}$$

$$\beta' = \text{atan} \frac{v}{U+u} \approx \frac{v}{U}$$

We can then insert the linearised aerodynamic coefficients and wind speed magnitude into the non-linear expressions (neglecting all higher order terms).

$$\vec{F}_{W'} = 1/2 \rho U^2 \left(\vec{C}_F(\bar{\alpha}, \bar{\beta}) + 2\vec{C}_F(\bar{\alpha}, \bar{\beta}) \frac{u}{U} + \partial_{\beta} \vec{C}_F(\bar{\alpha}, \bar{\beta}) \frac{v}{U} + \partial_{\alpha} \vec{C}_F(\bar{\alpha}, \bar{\beta}) \frac{w}{U} \right)$$

$$\vec{M}_{W'} = 1/2 \rho U^2 \left(\vec{C}_M(\bar{\alpha}, \bar{\beta}) + 2\vec{C}_M(\bar{\alpha}, \bar{\beta}) \frac{u}{U} + \partial_{\beta} \vec{C}_M(\bar{\alpha}, \bar{\beta}) \frac{v}{U} + \partial_{\alpha} \vec{C}_M(\bar{\alpha}, \bar{\beta}) \frac{w}{U} \right)$$

The dynamic wind aligned forces $\vec{F}_{W'}$ and moments $\vec{M}_{W'}$ were transformed to the static wind aligned forces \vec{F}_W and moments \vec{M}_W

$$\vec{F}_W = \mathbf{T}_{W' \rightarrow W} \cdot \vec{F}_{W'}$$

$$\vec{M}_W = \mathbf{T}_{W' \rightarrow W} \cdot \vec{M}_{W'}$$

$$\mathbf{T}_{W' \rightarrow W} = \begin{bmatrix} C\beta' C\alpha' & -S\beta' & -C\beta' S\alpha' \\ S\beta' C\alpha' & C\beta' & -S\beta' S\alpha' \\ S\alpha' & 0 & C\alpha' \end{bmatrix} \approx \begin{bmatrix} 1 & -v/U & -w/U \\ v/U & 1 & 0 \\ w/U & 0 & 1 \end{bmatrix}$$

The aerodynamic coefficients in the benchmark tests are based on 2D CFD analysis and will therefore only provide forces in the wind XZ-plane.

$$\begin{bmatrix} F_X \\ F_Y \\ F_Z \end{bmatrix}^W = \mathbf{T}_{W' \rightarrow W} \cdot \begin{bmatrix} F_X \\ 0 \\ F_Z \end{bmatrix}^{W'}$$

$$\begin{bmatrix} M_X \\ M_Y \\ M_Z \end{bmatrix}^W = \mathbf{T}_{W' \rightarrow W} \cdot \begin{bmatrix} 0 \\ M_Y \\ 0 \end{bmatrix}^{W'}$$

The static wind-aligned aerodynamic forces and moments are then expressed as

$$F_X = 1/2 \rho U^2 \left(C_{FX}(\bar{\alpha}, \bar{\beta}) + 2C_{FX}(\bar{\alpha}, \bar{\beta}) \frac{u}{U} + \partial_{\beta} C_{FX}(\bar{\alpha}, \bar{\beta}) \frac{v}{U} + \left(\partial_{\alpha} C_{FX}(\bar{\alpha}, \bar{\beta}) - C_{FZ}(\bar{\alpha}, \bar{\beta}) \right) \frac{w}{U} \right)$$

$$F_Y = 1/2 \rho U^2 \left(C_{FX}(\bar{\alpha}, \bar{\beta}) \frac{v}{U} \right)$$

$$F_Z = 1/2 \rho U^2 \left(C_{FZ}(\bar{\alpha}, \bar{\beta}) + 2C_{FZ}(\bar{\alpha}, \bar{\beta}) \frac{u}{U} + \partial_{\beta} C_{FZ}(\bar{\alpha}, \bar{\beta}) \frac{v}{U} + \left(\partial_{\alpha} C_{FZ}(\bar{\alpha}, \bar{\beta}) + C_{FX}(\bar{\alpha}, \bar{\beta}) \right) \frac{w}{U} \right)$$

$$M_X = -1/2 \rho U^2 \left(C_{MY}(\bar{\alpha}, \bar{\beta}) \frac{v}{U} \right)$$

$$M_Y = 1/2 \rho U^2 \left(C_{MY}(\bar{\alpha}, \bar{\beta}) + 2C_{MY}(\bar{\alpha}, \bar{\beta}) \frac{u}{U} + \partial_{\beta} C_{MY}(\bar{\alpha}, \bar{\beta}) \frac{v}{U} + \partial_{\alpha} C_{MY}(\bar{\alpha}, \bar{\beta}) \frac{w}{U} \right)$$

$$M_Z = 0$$

2.4 Implementation

A dynamic wind simulation in OrcaFlex is initiated with a *static analysis* in OrcaFlex in which the static wind load is applied together with gravity loads. The bridge coordinates in the statically deformed model are exported to a WindSim steering file for wind field generation. The wind load coordinates and the element types are exported to a HDF5 database. Based on additional user specified properties (wind profile, gust spectrum, coherence functions etc.) the wind time series in the wind load coordinates can be synthesized using Inverse Fast Fourier Transformation (IFFT) in WindSim. The resulting wind time series is then parsed into the HDF5 database. When running the dynamic simulation in OrcaFlex, the external wind function will have access to the instantaneous state of the simulation and the HDF5 file. Using this information, the external function calculates the instantaneous wind forces and moments in each wind load point and applies the loads directly on the model during simulation.

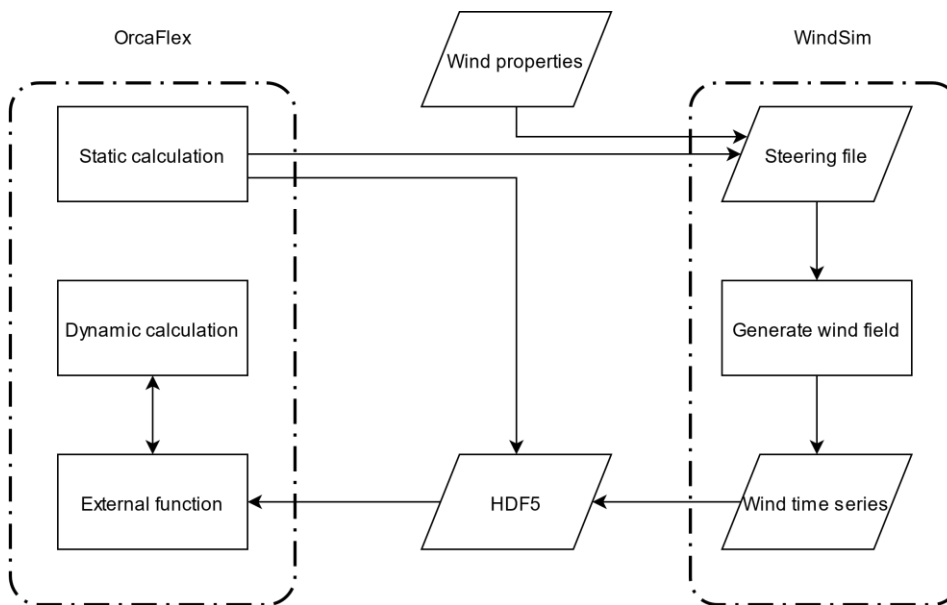


Figure 2-3: Flow chart of wind simulation in OrcaFlex

2.5 Assumptions

The theory implemented in the wind code are based on the following assumptions

- The bridge does not interfere with the wind field.
- The motions of the bridge are small, and it is assumed that the wind vectors in the static bridge state can be used during dynamic simulation.
- Self-excited aerodynamic forces are neglected.
- The aerodynamic coefficients are based on a steady-state CFD simulation. The coefficients are then applied to a unsteady simulation.
- The aerodynamic forces are based on a 2D assumption. This assumption may be questionable for large skew angles where 3D effects can be significant.

Hence, the results presented herein are to be considered indicative of the effect and not conclusive wr.t. design.

3 Benchmark

3.1 Model

The Bjørnafjorden K12 concept has been applied as a benchmark model for the skew wind study. In order to study the skew effect alone wind loads have only been applied on the bridge deck, and the aerodynamic coefficients are the same for all cross sections along the bridge girder. The mooring lines have for simplicity been represented with non-linear springs and dampers.

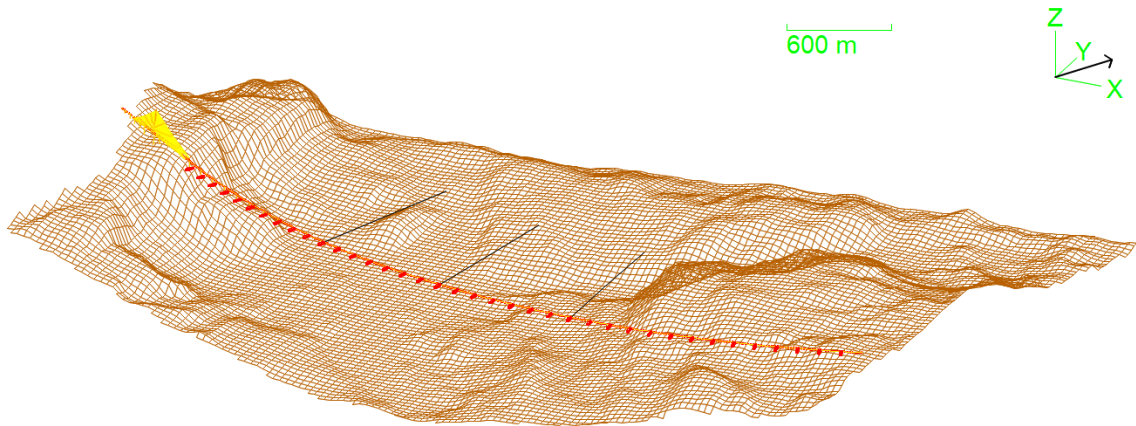


Figure 3-1: Bjørnafjorden K12 model

3.2 Aerodynamic coefficients

2D CFD simulations have been performed in RM Bridge using the *Discrete Vortex Method*. For each skew angle, a new cross section of the girder is subjected to simulations with varying angle of attacks.

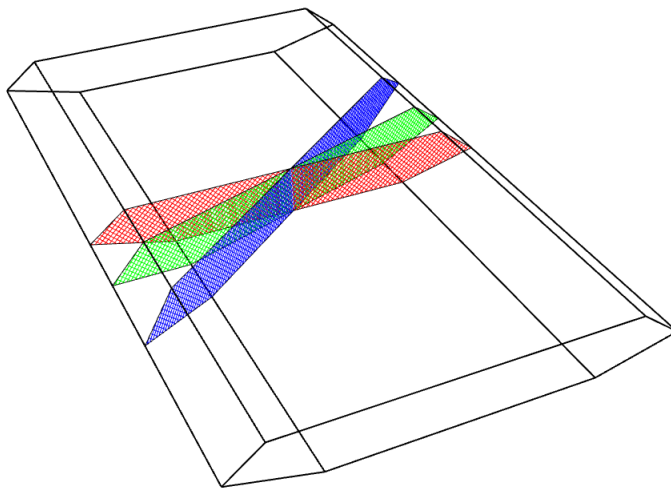


Figure 3-2:3 cross sections based on skew angle.

The resulting aerodynamic forces and moments is made non-dimensional with a constant width B and height H .

$$C_D = \frac{F_D}{\frac{1}{2} \rho H |U|^2}$$

$$C_L = \frac{F_L}{\frac{1}{2} \rho B |U|^2}$$

Skew wind sensitivity study

$$C_M = \frac{M}{\frac{1}{2}\rho B^2 |U|^2}$$

The static aerodynamic coefficients have been provided in the coordinate system shown below, and are shown in Figure 3-4 - Figure 3-6.

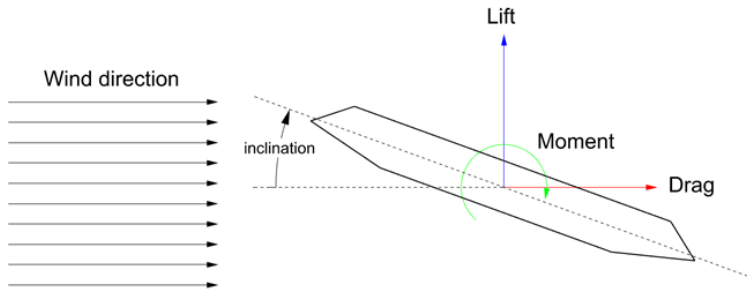


Figure 3-3: Aerodynamic coefficients definition

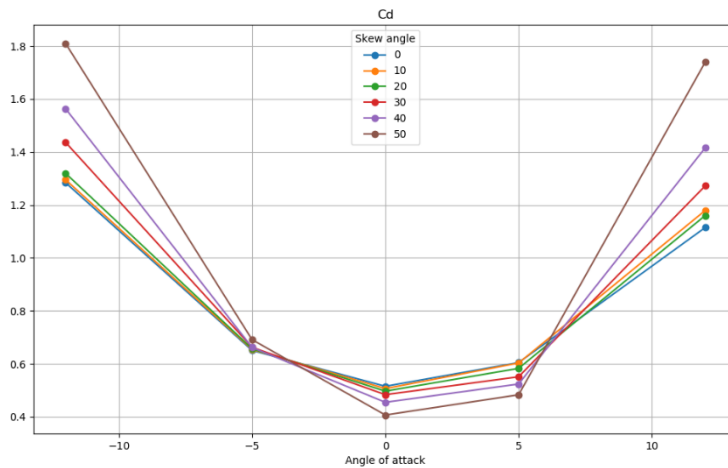


Figure 3-4: Drag coefficients

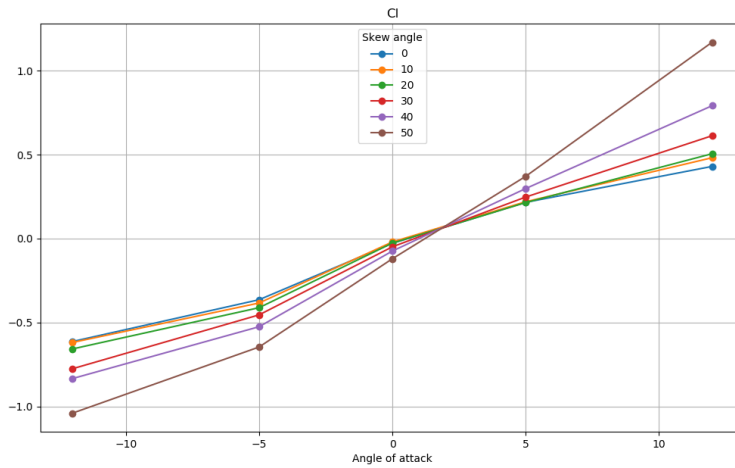


Figure 3-5: Lift coefficients

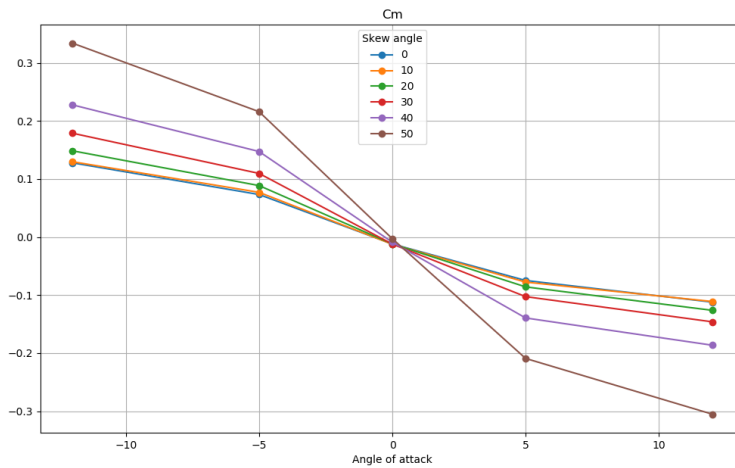


Figure 3-6: Moment coefficients

3.3 Analysis setup

To investigate the skew wind effect, three wind directions with equal wind field parameters has been simulated. Note that the wind direction is defined in the global coordinate system. 90 degrees as used below is then not directly perpendicular to the bridge axis (defined as the straight line between the bridge abutments), but has approximately a 10 degree offset.

Wind direction	60	90	120
Wind profile	N400	N400	N400
Basic wind speed	18.2 m/s	18.2 m/s	18.2 m/s
Surface roughness	0.01 m	0.01 m	0.01 m
Gust spectrum	N400	N400	N400
$I_U @ 10m$	14.5%	14.5%	14.5%
$I_V @ 10m$	12.2%	12.2%	12.2%
$I_W @ 10m$	8.7%	8.7%	8.7%
Coherence	N400	N400	N400
Duration	3600 s	3600 s	3600 s
Seeds	10	10	10

Three sets of OrcaFlex simulations have been performed:

1. 6 DOF model with aerodynamic coefficients as function of both skew angle and angle of attack.
2. 3 DOF model with aerodynamic coefficients as function of both skew angle and angle of attack.
3. 6 DOF model with aerodynamic coefficients as function of only angle of attack (Skew angle = 0).

3.4 Results

In the following the mean and standard deviations are given. The results are found from the time series subtracted the static response due to gravity, hence only giving the mean wind component and the standard deviation of the dynamic response due to wind.

In general, it is observed that a 3DOF skew wind applied load model sufficiently represents the wind responses in the bridge. The number of calls to the external wind code is therefore halved, which is a huge benefit with regards to computation time.

The Frequency Domain Decomposition method for output-only system identification has been applied to identify the contributing modes from the result time series.

3.4.1 Axial force

Skew wind coefficients increase the mean and fluctuating responses for all three wind directions investigated. The relative contribution from mode 9 (9.5 s) seems to increase for wind direction 120.

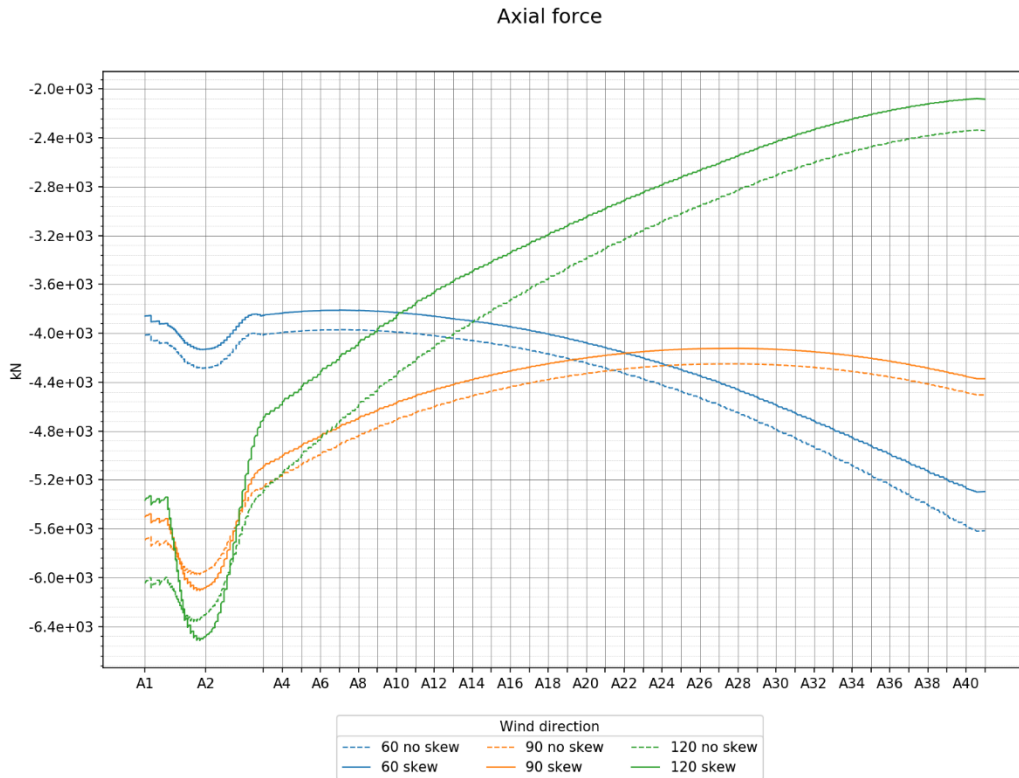


Figure 3-7: Mean axial force (skew vs non-skew)

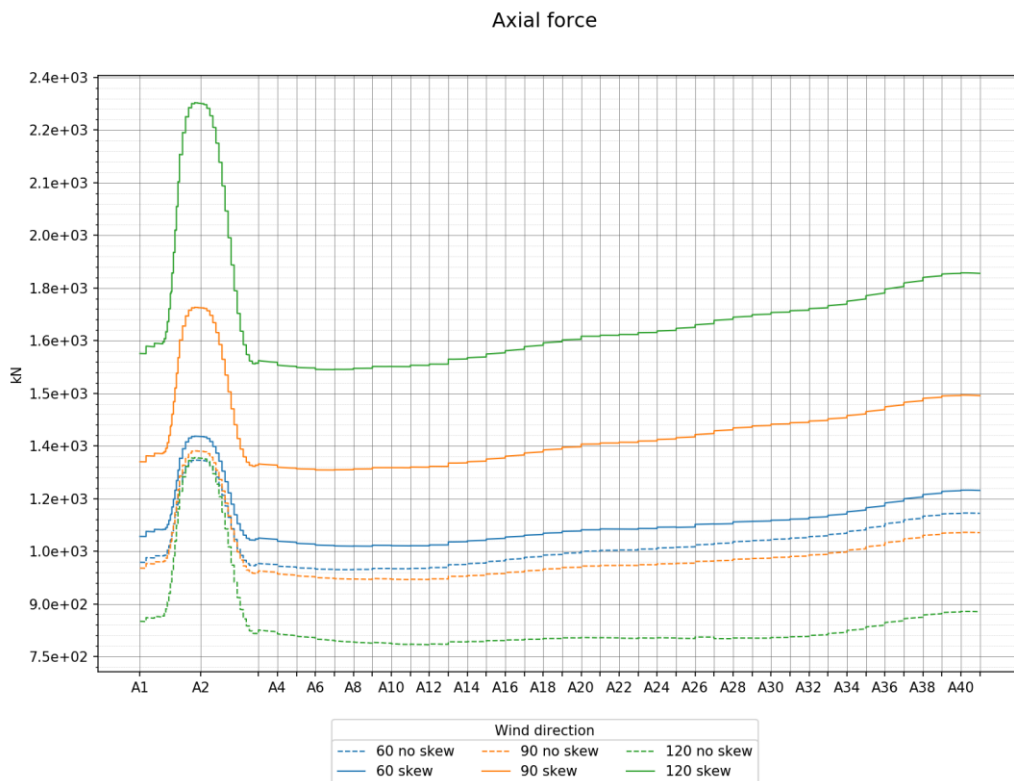


Figure 3-8: Standard deviation axial force (skew vs non-skew)

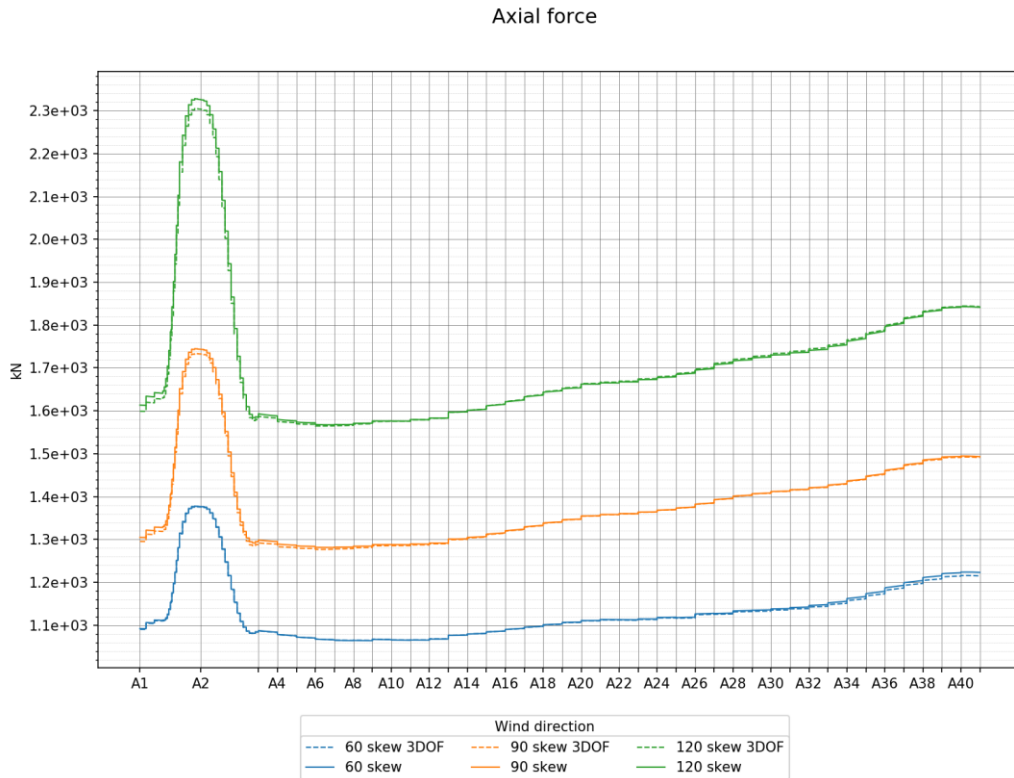


Figure 3-9: Standard deviation axial force (3DOF vs 6DOF)

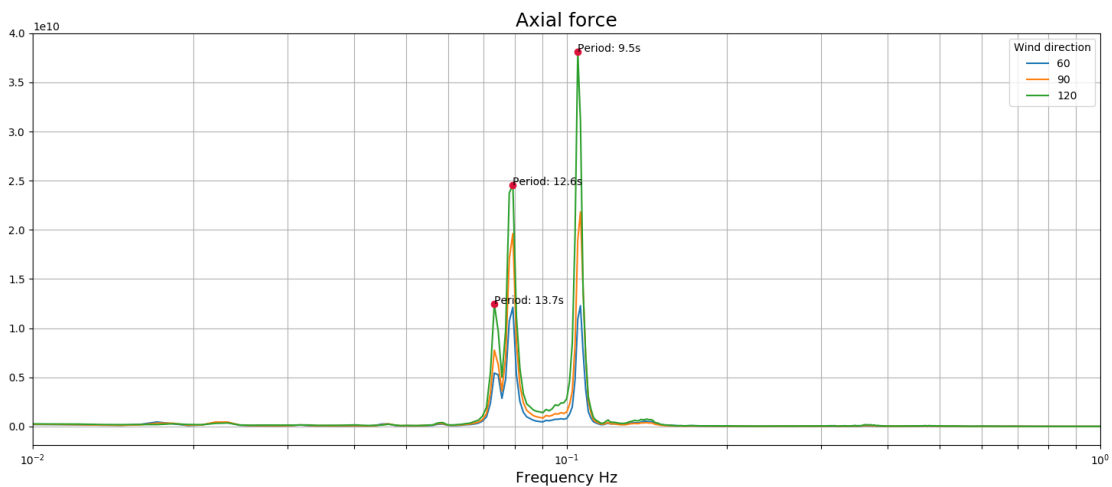


Figure 3-10: Axial force system identification

3.4.2 Strong axis bending moment

The skew wind effect on mean wind response is quite low. For the fluctuating response, lower dominating modes (1,2 and 3) are excited more by wind direction 60 and 90, while higher dominating modes (5,7 and 9) are excited more by wind direction 120.

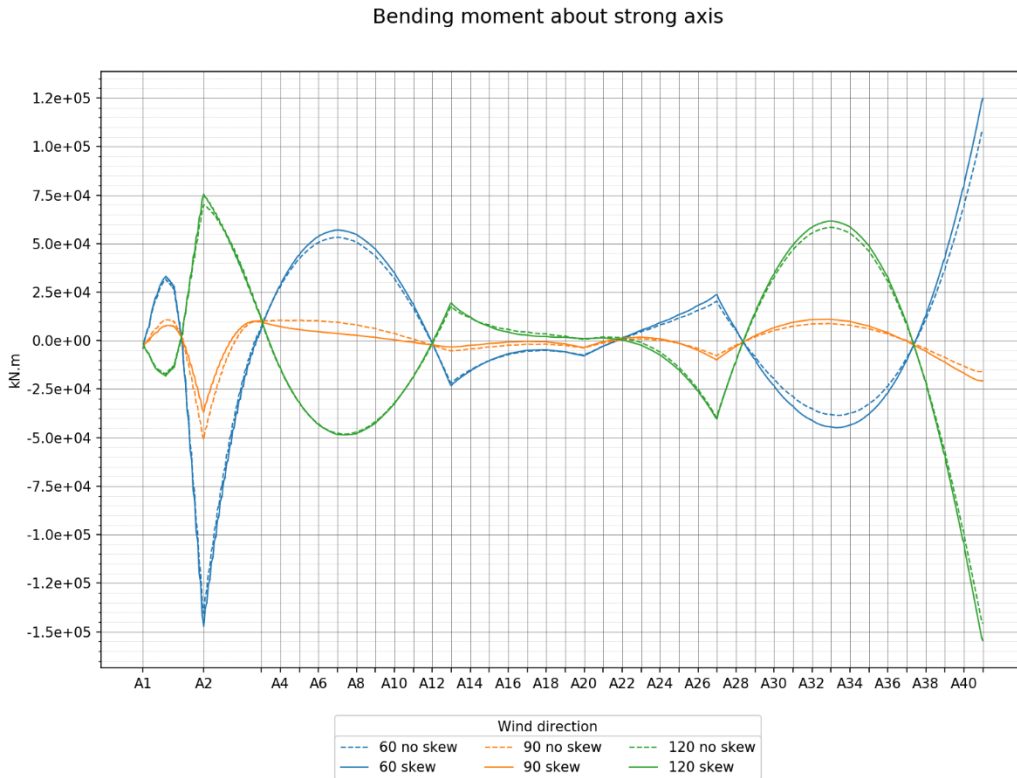


Figure 3-11: Mean strong axis bending moment (skew vs non-skew)

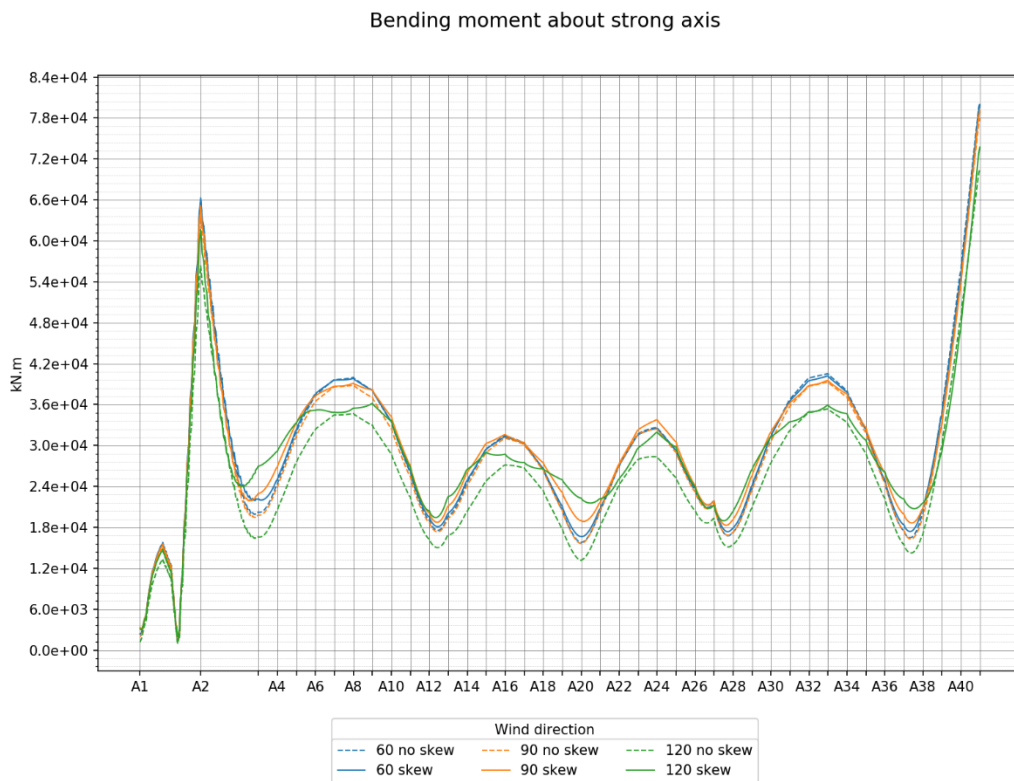


Figure 3-12: Standard deviation strong axis bending moment (skew vs non-skew)

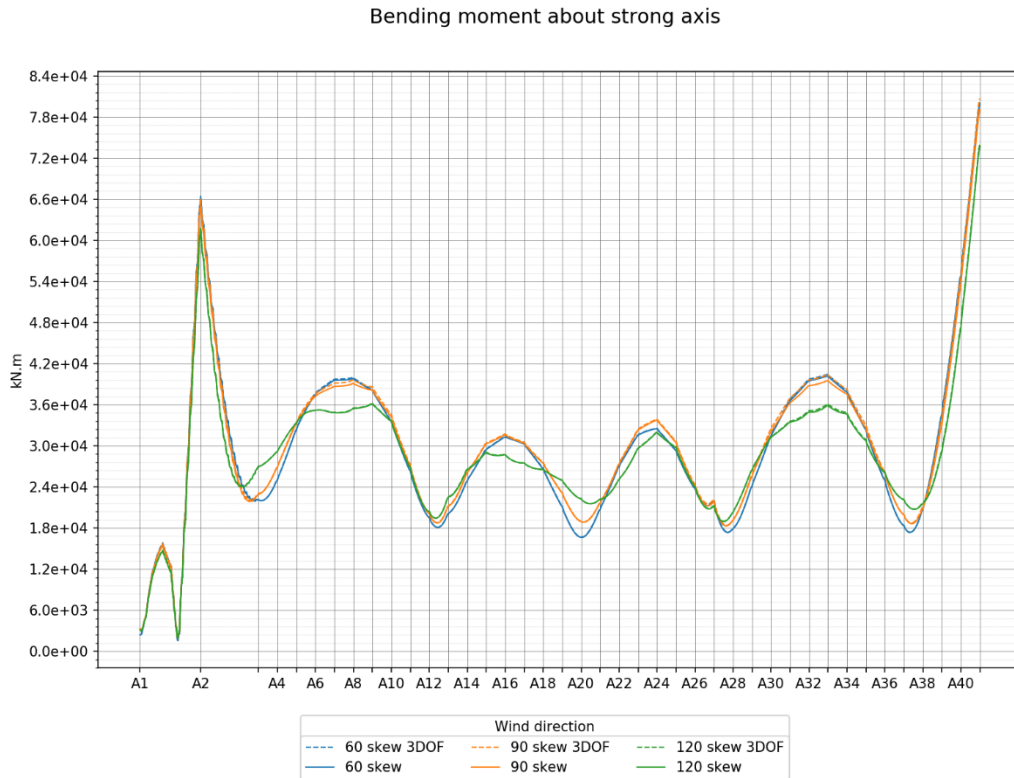


Figure 3-13: Standard deviation strong axis bending moment (3DOF vs 6DOF)

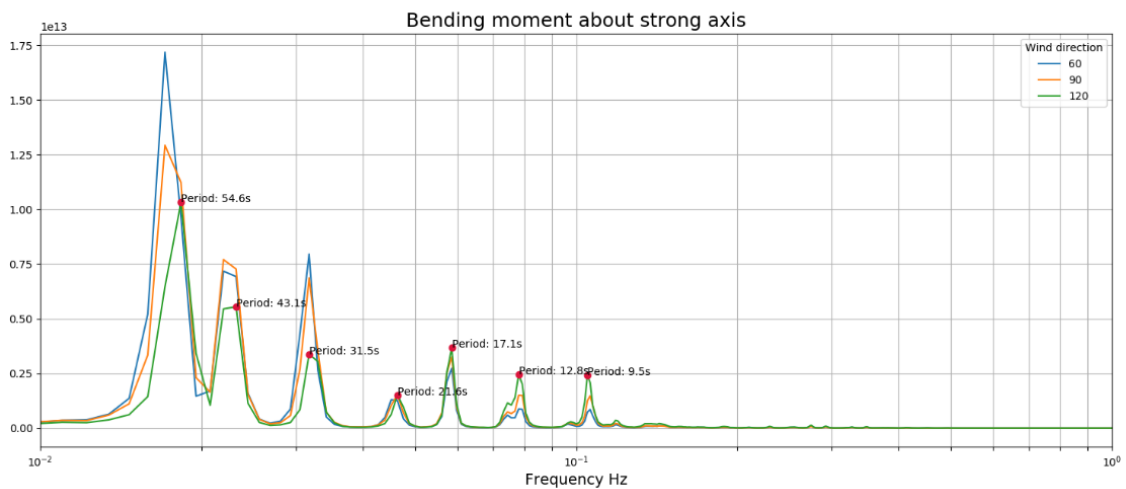


Figure 3-14: Strong axis bending moment system identification

3.4.3 Weak axis bending moment

The skew wind effect is mostly important from A2 to A14. For wind direction 60, the dynamic response and the skew wind angle is high at the north end of the bridge, and vice versa for wind direction 120. It is therefore reasonable to believe that these observations are correlated. The response is related to excitation of higher modes around 3.5 s and 2.7 s.

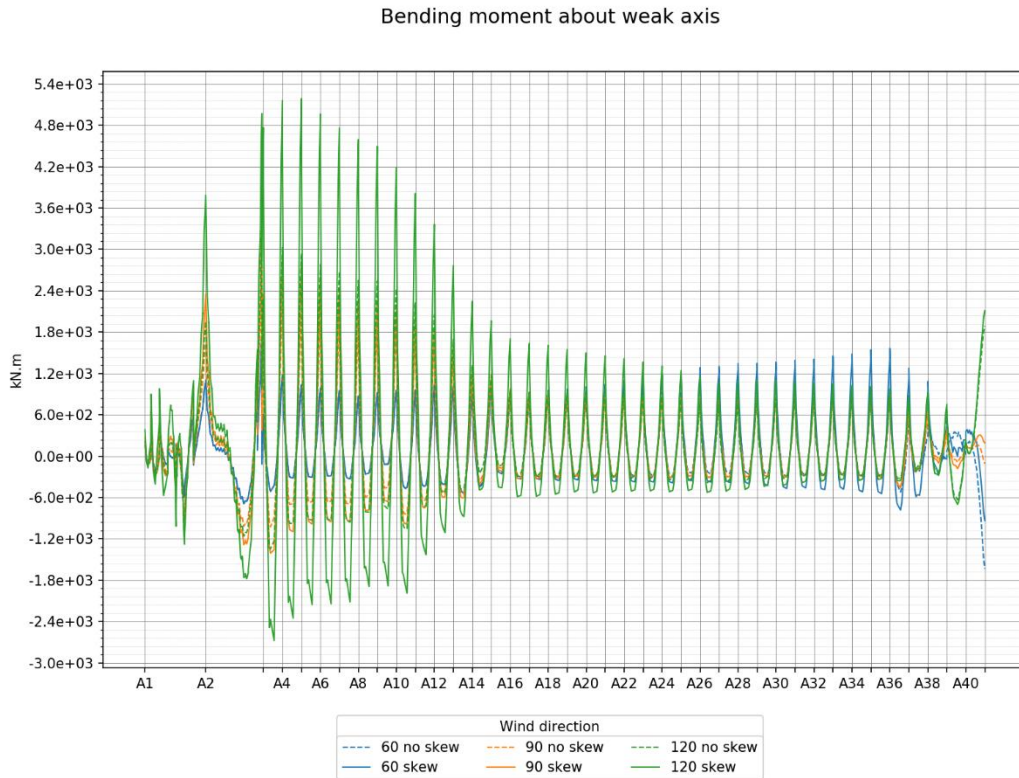


Figure 3-15: Mean weak axis bending moment (skew vs non-skew)

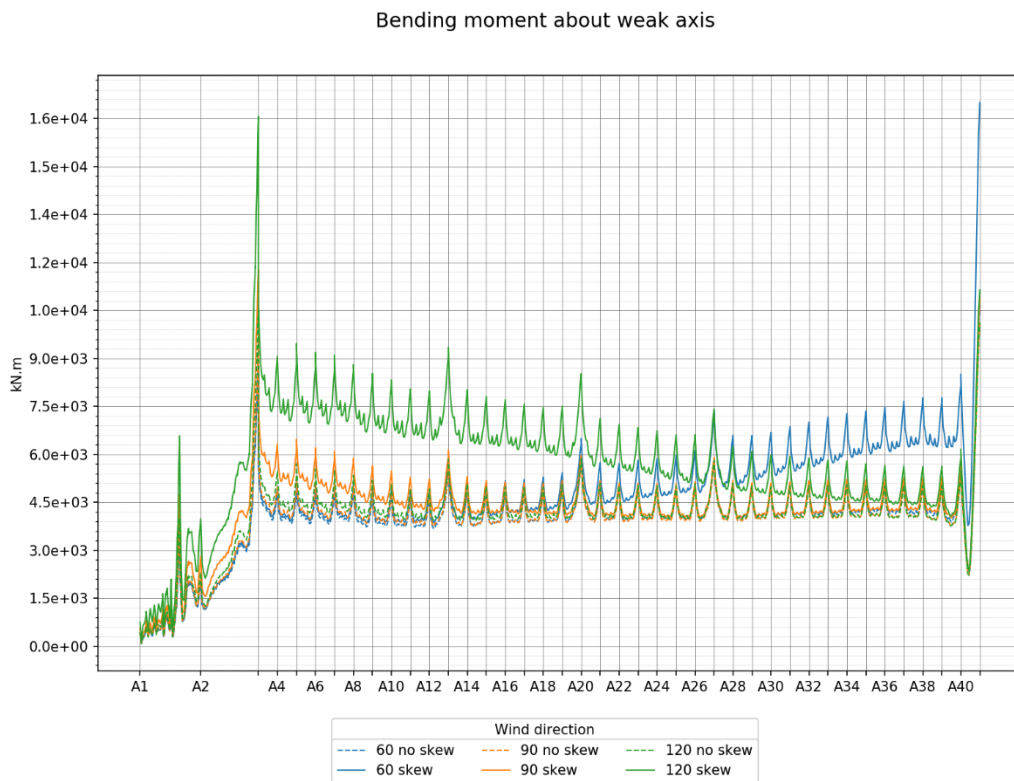


Figure 3-16: Standard deviation weak axis bending moment (skew vs non-skew)

Bending moment about weak axis

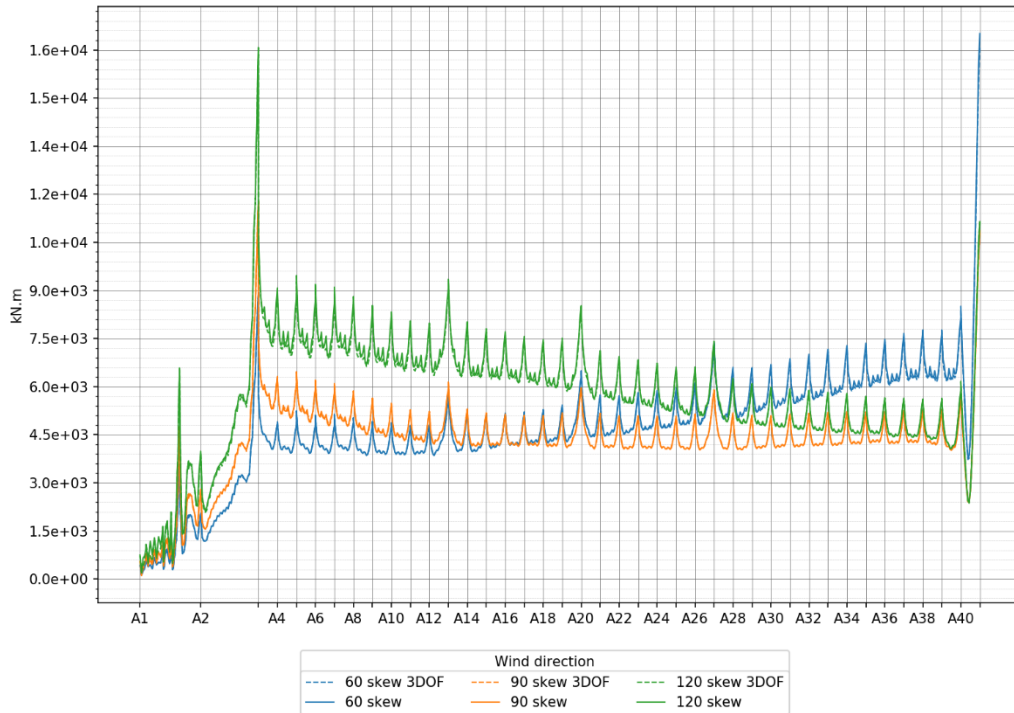


Figure 3-17: Standard deviation weak axis bending moment (3DOF vs 6DOF)

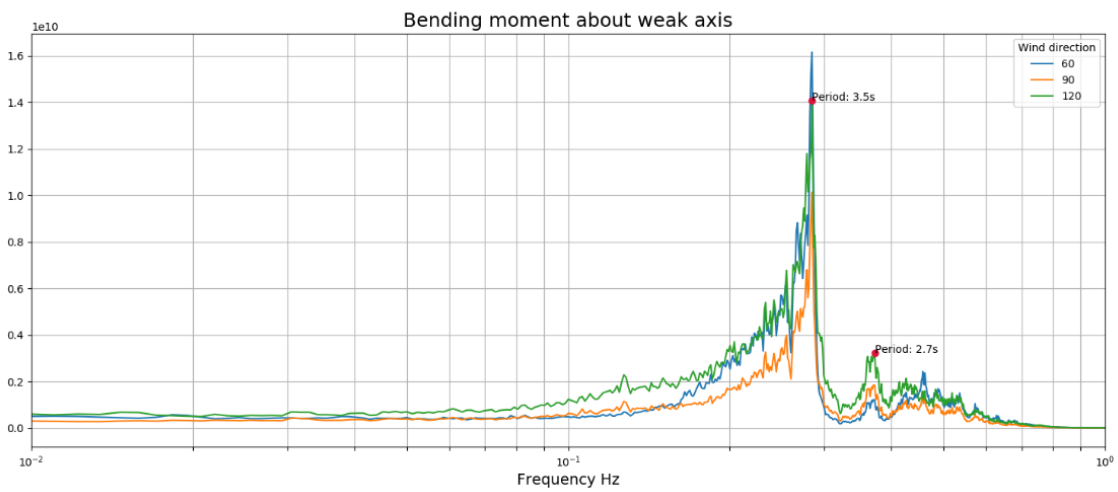


Figure 3-18: Weak axis bending moment system identification

3.4.4 Torsional moments

The skew wind effect is most dominant for wind direction 120. Mode 1 is more important is more excited in wind direction 60. For the other modes, wind direction 90 and 120 is more excited. Contributing modes in torsional moments span from mode 1 (55 s) up to higher modes (around 3 s)

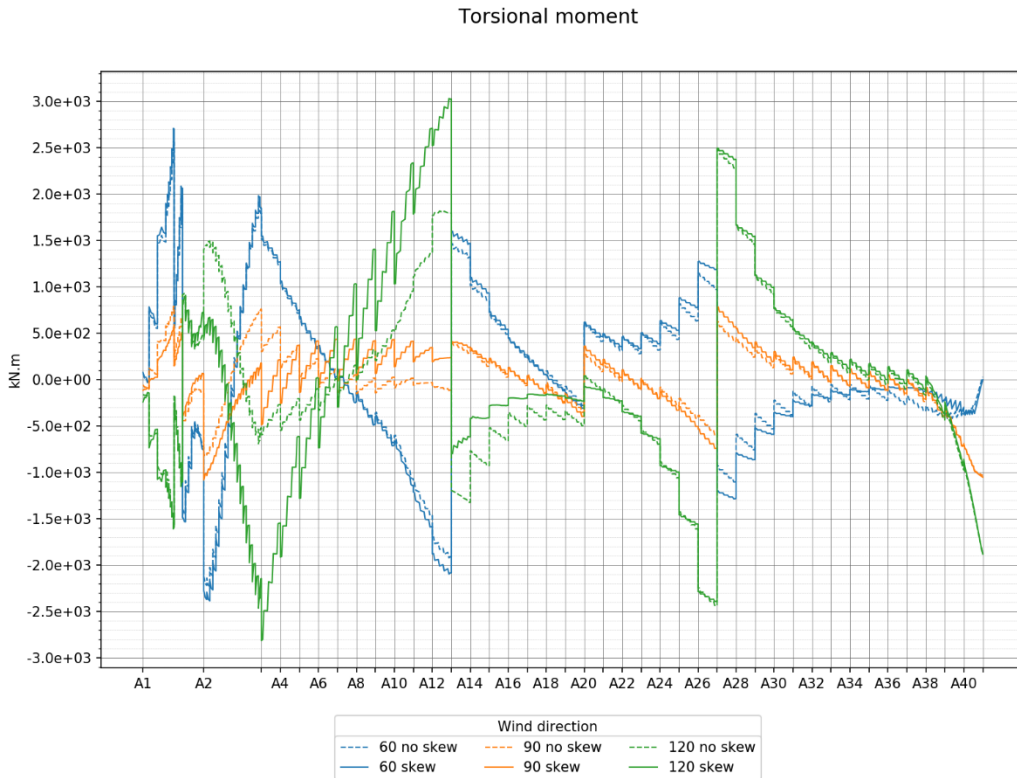


Figure 3-19: Mean torsional moment (skew vs non-skew)

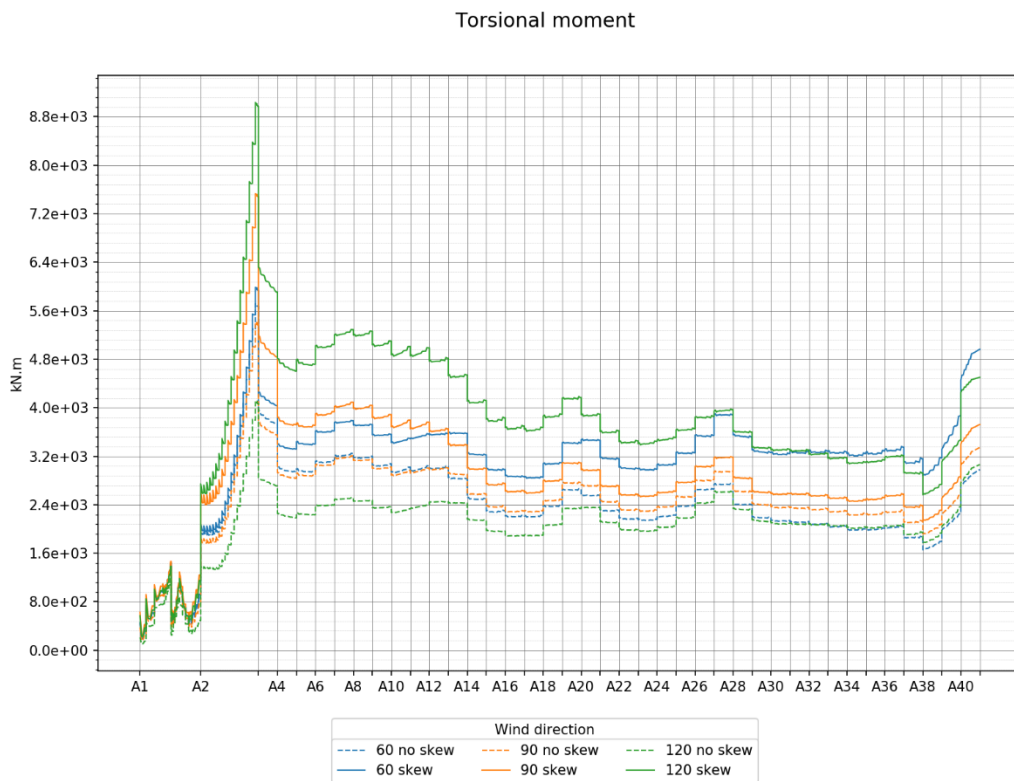


Figure 3-20: Standard deviation torsional moment (skew vs non-skew)

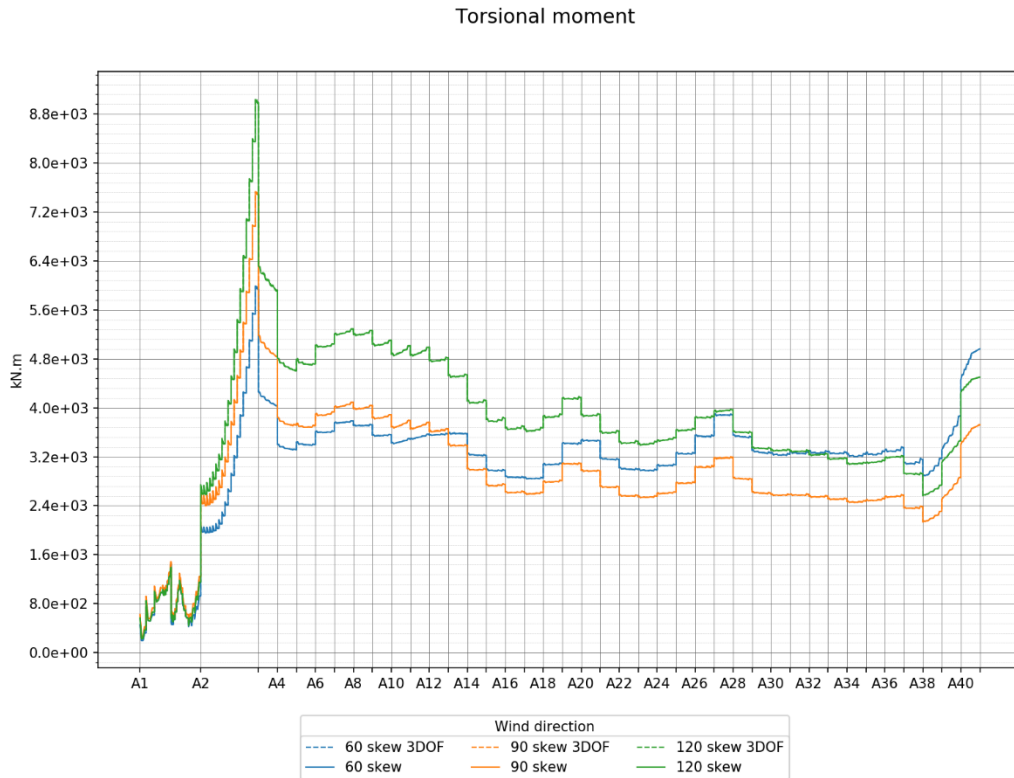


Figure 3-21: Standard deviation torsional moment (3DOF vs 6DOF)

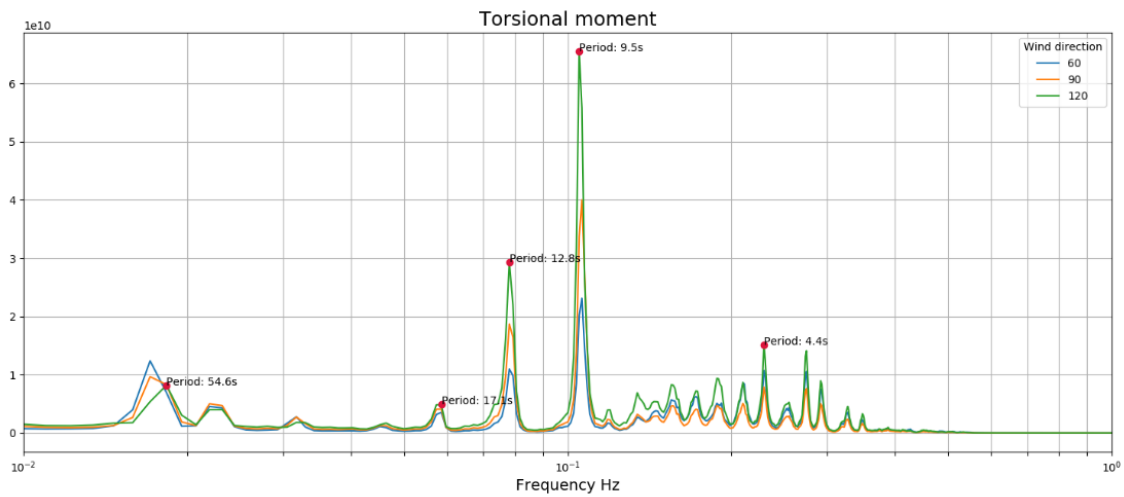


Figure 3-22: Torsional moment system identification